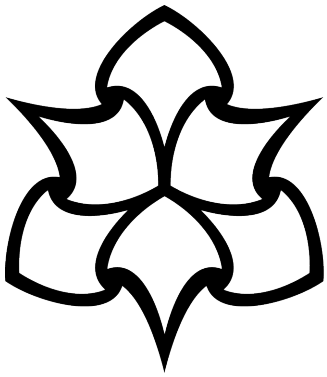

Manuscript Details

Manuscript number	EXG_2019_287_R2
Title	Morphological alterations of mouse skeletal muscles during early ageing are muscle specific
Article type	Research Paper

Abstract

One of the hallmarks of ageing is muscle wasting that may be preceded by morphological changes, such as capillary rarefaction. Muscle-specific changes in morphology in early ageing may differ between locomotor and respiratory muscles. To investigate this, we compared capillarization, fiber type composition, fiber cross-sectional area (FCSA) and oxidative capacity of individual fibers of the soleus (n=6/5 for 20- and 79 weeks, respectively), extensor digitorum longus (EDL: n=3/3) and diaphragm (n=7/5) muscles in 20- (mature) and 79-week-old (early ageing) CD-1 female mice. There was no significant loss of soleus and EDL mass. The FCSA was larger and the capillary density lower at 79 than 20 weeks in the diaphragm, while in the EDL the opposite was found (both $p \leq 0.002$) with no significant ageing-related differences in the soleus. The heterogeneity in capillary spacing, which may negatively impact on muscle oxygenation, was highest in muscles from 20-week-old mice, irrespective of muscle ($p \leq 0.011$). Succinate dehydrogenase activity, indicative of oxidative capacity, and capillary to fiber ratio did not significantly change with age in any muscle. At all ages, the capillary supply to a fiber was positively related to FCSA in each muscle. We conclude that despite previously reported early age-related reductions in specific tension in both locomotor and respiratory muscles, morphological changes show a muscle-specific pattern in early ageing CD-1 mice. Specifically, early aging was associated with 1) diaphragm hypertrophy 2) and fiber atrophy in the EDL that was not accompanied by angiogenesis, capillary rarefaction or reductions in oxidative capacity.

Keywords	Aging, Maturation, Capillarization, Oxidative capacity, Skeletal muscle, Capillary Domain
Manuscript category	Musculoskeletal System and Exercise

Corresponding Author	Hans Degens
Corresponding Author's Institution	Manchester Metropolitan University
Order of Authors	Guy Messa, Mathew Piasecki, Cameron Hill, Jamie McPhee, Jason Tallis, Hans Degens
Suggested reviewers	Antonios Matsakas, Arimantas Lionikas, Dawn Lowe, Stephen Alway, Stuart Gray

Submission Files Included in this PDF

File Name [File Type]

190712responsetoreviewers.docx [Response to Reviewers]

190611Highlights.docx [Highlights]

190712AAGEINGEXPERIMENTALGERONTOLOGYr2.docx [Manuscript File]

To view all the submission files, including those not included in the PDF, click on the manuscript title on your EVISE Homepage, then click 'Download zip file'.

Research Data Related to this Submission

There are no linked research data sets for this submission. The following reason is given:
Data will be made available on request

We thank reviewer 1 for additional comments to improve the manuscript and remove a mistake from the manuscript. The small changes we made are indicated in red in the text.

1) PAGE 5: CD-1 are outbred mice, and the authors describe their advantages in comparison to inbred strains. However, in the second line from the bottom these mice are referred to as a strain. A strain is produced by repeated brother sister mating for 20 generations or more, hence an inbred strain terminology. The CD-1 mice certainly were not generated in that way, therefore they should be referred to as outbred mice, or just CD-1 mice.

Response: We thank the reviewer for this comment and we now refer to these mice as just CD-1 mice.

2) The authors replaced some abbreviations and that should be congratulated. Yet many more than needed were retained in the text (also in the figures). It is regretable that the authors elected to prioritise teaching potential readers new terminology instead of using common vocabulary to make their message accessible to as broad readership as possible.

Response: We have followed up this suggestion and also replaced in the figures 'DIA' and 'SOL' with 'Diaphragm' and 'Soleus', respectively. Concerning abbreviations as SDH, SDH-INT, LCFR and CFD; we felt we needed to keep these as spelling out these abbreviations does not help readability. To accommodate the unusual abbreviations we defined them in the discussion again.

It should also be noted that these parameters can not just be replaced with the more commonly used capillary to fibre ratio (C:F) and capillary density (CD) that reflect overall indicators of muscle capillarisation. In contrast, our parameters are specific for individual fibres, we feel a crucial difference that deserves indeed 'teaching potential readers new terminology' as it are new parameters providing more detailed information on capillarisation and oxidative capacity in the muscle than the conventional parameters.

Highlights

In CD-1 mice early ageing was associated with hypertrophy of diaphragm and atrophy of extensor digitorum longus muscle fibers

The diaphragm hypertrophy and atrophy in the EDL were not accompanied by angiogenesis, capillary rarefaction or reductions in oxidative capacity

Ageing-related changes differ between muscles

Morphological alterations of mouse skeletal muscles during early ageing are muscle specific

Messa GAM[a], Piasecki M[b], Hill C[c,d], McPhee JS[e], Tallis J[d], Degens H[a,f,g]

[a] School of Healthcare Science, Research Centre for Musculoskeletal Science & Sports Medicine, Manchester Metropolitan University, UK

[b] Clinical, Metabolic and Molecular Physiology, MRC-ARUK Centre for Musculoskeletal Ageing Research and National Institute for Health Research (NIHR) Nottingham Biomedical Research Centre, University of Nottingham, UK

[c] Randall Centre for Cell and Molecular Biophysics, New Hunt's House, Guy's Campus, Kings College, London, UK

[d] Center for Sport, Exercise and Life Sciences, Alison Gingell Building, Coventry University, Priory Street, Coventry CV1 5FB, UK

[e] Department of Sport and Exercise Sciences, Research Centre for Musculoskeletal Science & Sports Medicine, Manchester Metropolitan University, UK

[f] Institute of Sport Science and Innovations, Lithuanian Sports University, Lithuania

[g] University of Medicine and Pharmacy of Targu Mures

Address for correspondence:

Prof Hans Degens

School of Healthcare Science

Manchester Metropolitan University

John Dalton Building; Chester Street

Manchester M1 5GD

United Kingdom

Phone: +44.161.247.5686

E-mail: h.degens@mmu.ac.uk

Abstract

One of the hallmarks of ageing is muscle wasting that may be preceded by morphological changes, such as capillary rarefaction. Muscle-specific changes in morphology in early ageing may differ between locomotor and respiratory muscles. To investigate this, we compared capillarization, fiber type composition, fiber cross-sectional area (FCSA) and oxidative capacity of individual fibers of the soleus (n=6/5 for 20- and 79 weeks, respectively), extensor digitorum longus (EDL: n=3/3) and diaphragm (n=7/5) muscles in 20- (mature) and 79-week-old (early ageing) CD-1 female mice. There was no significant loss of soleus and EDL mass. The FCSA was larger and the capillary density lower at 79 than 20 weeks in the diaphragm, while in the EDL the opposite was found (both $p \leq 0.002$) with no significant ageing-related differences in the soleus. The heterogeneity in capillary spacing, which may negatively impact on muscle oxygenation, was highest in muscles from 20-week-old mice, irrespective of muscle ($p \leq 0.011$). Succinate dehydrogenase activity, indicative of oxidative capacity, and capillary to fiber ratio did not significantly change with age in any muscle. At all ages, the capillary supply to a fiber was positively related to FCSA in each muscle. We conclude that despite previously reported early age-related reductions in specific tension in both locomotor and respiratory muscles, morphological changes show a muscle-specific pattern in early ageing CD-1 mice. Specifically, early aging was associated with 1) diaphragm hypertrophy 2) and fiber atrophy in the EDL that was not accompanied by angiogenesis, capillary rarefaction or reductions in oxidative capacity.

Keywords: Aging, Maturation, Capillarization, Oxidative capacity, Skeletal muscle

Introduction

With increasing age, mammals progressively lose muscle mass (referred to as sarcopenia) and strength. This weakness and loss of muscle mass has been attributed to a loss of fibers, preferential type II atrophy and a reduction in specific tension (Andersen 2003; Barnouin et al., 2017; Degens and Korhonen 2012; Fragala et al., 2015; Larsson et al., 2019; Lexell et al., 1988; McPhee et al., 2018). In addition to muscle weakness, older muscle may also suffer from an earlier onset of muscle fatigue, particularly during repeated and shortening contractions (Allman and Rice 2002; Callahan and Kent-Braun 2011). The consequences of progressive weakness are many and varied and together contribute significantly to frailty, reduced mobility and quality of life, often leading to the loss of independence and social isolation (McPhee et al., 2016). To develop effective countermeasures, it is important to improve understanding of the effects of ageing on skeletal muscle. In addition, recognizing early signs of sarcopenia will help inform preventative measures.

In previous studies it has been shown that ageing-related muscle weakness in humans is a consequence of both loss of muscle mass and a reduction in force or power per muscle cross-sectional area (McPhee et al., 2018). In mice, an ageing-related reduction in specific tension has been reported for both locomotor and diaphragm muscles (Ballak et al., 2014; Chan and Head 2010; Hill et al., 2018), in many cases such age related changes occur in the absense of muscle (fiber) atrophy. This indicates that a reduction in specific tension may well be an early hallmark of ageing.

Different muscles may show different ageing-related changes. For instance, whilst quadriceps strength is reduced by almost 40% between the 2nd and 7th decade of life (Klitgaard et al., 1990; McPhee et al., 2018; Young et al., 1985), the strength of the diaphragm is reduced by about 25% over the same period (Polkey et al., 1997; Tolep et al., 1995). Furthermore, in contrast to the locomotor muscles (Allman and Rice 2002; Degens and Alway 2006; Degens and Veerkamp 1994), there is some evidence that diaphragm fatigability is unaltered with age in humans (Polkey et al., 1997; Tolep et al., 1995) or even elevated, at least during early ageing, in mice (Tallis et al., 2014). In addition to different patterns of use related to different functional requirements, an increased load on the diaphragm due to the ageing-related increase in chest wall stiffness (Teramoto et al., 1995) may offer protection to the diaphragm from the effects of disuse and ageing.

Besides a loss of muscle strength, also other ageing-related changes occur, such an ageing-related reduction in oxidative capacity that is proportionally larger than the loss of capillaries, resulting in a capillarization in relative excess to the oxidative capacity of muscle fibers in the soleus and white region of the rat gastrocnemius muscle (Hepple and Vogell 2004). These muscles also showed atrophy, while in the red region of the gastrocnemius, where fiber hypertrophy occurred, there was no excessive capillarization (Hepple and Vogell 2004). These data indicate that the effects of ageing on muscle morphology may differ between muscles, and it remains to be seen if excessive capillary supply and loss of oxidative capacity are early hallmarks of ageing.

The significance of capillaries for oxygen supply to mitochondria is demonstrated by the fact that muscles or muscle regions with a high oxidative capacity have a denser capillary network than those with low oxidative capacity (Degens et al., 1992; Larsson et al., 2019). Yet, the number of capillaries supplying a fiber is more strongly associated with fiber size than with fiber type (Ahmed et al., 1997) or oxidative capacity (Bosutti et al., 2015). This intricate interrelationship between size and the capillary supply to a fiber is also indicated by the proportional (Green et al., 1999) and similar temporal (Holloway et al., 2018) increase in capillary number and fiber size in the quadriceps after 12 weeks resistance training in young men, and the similar time course of muscle fiber hypertrophy and capillary proliferation in rat models of compensatory hypertrophy (Egginton et al., 2011; Plyley et al., 1998). It has been suggested that the ageing-related muscle atrophy may be preceded by capillary loss (Larsson et al., 2019).

Although the distribution of capillaries has a significant impact on tissue oxygenation (Degens et al., 2006; Degens et al., 1994), it is rarely considered in studies on the effects of ageing on muscle capillarization. The absence of any significant changes in the heterogeneity of capillary spacing during maturational (Degens et al., 2006) or hypertrophic muscle growth (Degens et al., 1992), suggest that the neoformation of capillaries is a controlled process. There is, however, some indication that the heterogeneity of the capillary spacing was higher in 5- than 25-month-old rat plantaris muscle, which was linked to the increased heterogeneity in fiber size (Degens et al., 2009). Given that there is a lower heterogeneity in capillary spacing in slow oxidative than fast muscles (Egginton et al., 1988), it remains to be seen whether there are any muscle-specific effects of early ageing on the heterogeneity of capillary spacing in slow-oxidative and fast-glycolytic limb muscles, and the diaphragm.

Another part of the ageing-related decrement in specific tension is attributable to intermuscular fat infiltration (Delmonico et al., 2009; Hogrel et al., 2015). Also, intramyocellular lipid (IMCL) content may increase (Rahemi et al., 2015; Schwenzer et al., 2009) and modelling data indicate that this would further contribute to the lower specific tension in old age (Rahemi et al., 2015). Besides the effect of a larger IMCL content at the expense of myofibrils, apoptosis induced by intracellular lipids via elevated oxidative stress (Kob et al., 2015) may further contribute to the decreased specific tension. However, information about changes in IMCL content during ageing is lacking and may be muscle specific, as suggested by a larger accumulation of IMCL after a high fat diet + denervation in mouse soleus than extensor digitorum longus (EDL) muscle fibers (Komiya et al., 2017).

The aim of the present study was to investigate the effects of early ageing on skeletal muscle morphology and more specifically the relationship between the fiber capillary supply with fiber type, size, oxidative capacity and IMCL in a postural slow oxidative muscle (the soleus), a muscle that is intermittently active (the fast, more glycolytic EDL) and a muscle that is constantly active (the diaphragm, highly oxidative with a mixed fiber type composition). It was hypothesized that early-ageing-related changes in muscle morphology occur in the absence of significant atrophy and are more pronounced in locomotor muscles than in the diaphragm.

Materials and methods

Animals

The effects of early ageing on skeletal muscle may be masked by maturational changes when using not fully-matured animals as the control group. An example of this masking of ageing effects is the absence of a difference in force generating capacity between the plantaris muscles from 5- and 25-month-old rats, while there was a significant reduction between the age of 13 and 25 months (Degens et al., 1993a). Since the mass of the extensor digitorum longus muscle (EDL) was higher in 30- than 10-week-old CD-1 mice and specific tension lower (Tallis et al., 2014), we have chosen 20-week-old CD-1 mice in the present study as the fully matured young-adult group to minimize bias of maturation and 79-week-old mice representing early ageing, as they already show a reduction in specific tension, but without loss of muscle mass (Hill et al., 2018). CD-1 mice were selected as it is outbred enough to display a genetic heterogeneity similar to that found in humans (Aldinger et al., 2009; Rice and Obrien 1980), thus replicating

the genetic heterogeneity found in humans more closely than inbred strains as the C57BL/6J mouse.

Fifty-nine female CD-1 mice (Charles River Ltd., Harlan, UK), housed 8-10 per cage at Coventry University, were maintained on a 12/12 h light/dark cycle at 20-22°C. They were fed *ad libitum* a low-fat standard chow diet (CRM(P); SDS/Dietex International Ltd, Whitham, UK; calories provided by protein 17.49%, fat 7.42%, carbohydrate, 75.09%; gross energy 3.52 kcal/g; metabolizable energy 2.57 kcal/g). At the age 20 or 79 weeks, animals were weighed, sacrificed by cervical dislocation [in accordance with British Home Office Animals (Scientific Procedures) Act 1986, Schedule 1] and then snout-to-anus length was determined using digital callipers (Fisher Scientific™ 3417, Fisher Scientific, Loughborough, UK) to calculate the body mass index (BMI) as body mass (kg) divided by snout-to-anus length (cm) squared (Hill et al., 2019; Sjogren et al., 2001). All experimental procedures were carried out in compliance with the local ethical review board of Coventry University.

The removal of the soleus (20 w: n = 6; 79 w: n = 5), extensor digitorum longus (EDL; 20w: n = 3; 79w: n = 3) and right part of the diaphragm (20 w: n = 7; 79 w: n = 5) muscles were performed as outlined by (Tallis et al., 2017). After excision, the muscles were blotted dry and weighed (except the diaphragm, as only strips were excised), embedded in Tissue-Tek optimal cutting temperature freezing medium (Leica Biosystems, Nußloch, Germany), frozen in liquid-nitrogen-cooled isopentane (Sigma Aldrich, Steinheim, Germany) and stored at -80°C until use.

Histological analysis and microscopy

Serial 10-µm thick cross-sections of the soleus, EDL and diaphragm muscles were cut with a cryostat (CM3050S; Leica, Nußloch, Germany) at -21°C and collected on Superfrost Plus microscope slides. Serial sections were stained for intramyocellular lipid (IMCL), myosin heavy chain (MHC), capillaries, or succinate dehydrogenase (SDH).

Intramyocellular fat. Sudan Black B was used to stain IMCL. The Sudan Black B dye stains mainly neutral lipids (mainly triglycerides) with a blue-black tint. Briefly, air-dried sections were fixed in 10% formalin for 10 min. Sections were then washed three times for 1 min in distilled water before incubation in propylene glycol for 3 min. Sections were then incubated in the Sudan Black B solution (preheated at 60°C) for 7 min, differentiated in 85% propylene

glycol for 3 min and subsequently washed three times for 1 min in distilled water. Sections were cover-slipped using glycerol gelatin.

Fiber typing. Serial sections were immunohistochemically stained for type I, IIa, IIx or IIb MHC using mouse monoclonal primary antibodies BA-D5 (1 $\mu g \cdot mL^{-1}$), SC-71 (1 $\mu g \cdot mL^{-1}$), 6H1 (10 $\mu g \cdot mL^{-1}$) and BF-F3 (5 $\mu g \cdot mL^{-1}$), respectively (Development Studies Hybridoma Bank, Iowa, USA). One section was co-stained for type I, IIa and IIx MHC and a serial section for type IIb MHC.

Sections were fixed with ice-cold acetone for 15 min and then blocked for 45 min with 10% goat serum in phosphate-buffered saline (PBS) at room temperature. Following a wash with PBS, the sections were incubated with the primary antibody for 90 min in a humid chamber. The sections were subsequently washed in PBS and incubated in the dark for 60 min with Alexa 350 IgG anti-mouse (2 $\mu g \cdot mL^{-1}$, Invitrogen, UK) or Alexa 488 IgG anti-mouse (2 $\mu g \cdot mL^{-1}$, Invitrogen, UK) for type I and IIa fibers, respectively and Alexa 555 IgG anti-mouse (2 $\mu g \cdot mL^{-1}$ Invitrogen, UK) for type IIx and IIb fibers. Sections were washed, dried and mounted using Prolong Diamond antifade mounting medium (Life Technologies, UK). Sections without the primary antibodies served as negative controls. Images were taken with a Carl Zeiss AxioMRc Camera (Gottingen, Germany) on a Zeiss fluorescence microscope (10x objective).

Succinate dehydrogenase. The succinate dehydrogenase (SDH) activity was assessed according to the protocol described by Wüst et al., (2009). Sections were incubated for SDH in 37.5 mM sodium phosphate buffer (pH 7.6), 74 mM sodium succinate and 0.4 mM tetranitro blue tetrazolium in the dark at 37°C for 20 min. The reaction was stopped with 0.01 N HCl for 10 s. The slides were then washed with two changes of distilled water, mounted in glycerol gelatin and stored in the dark until measurement of the staining intensity within two days. All samples were processed simultaneously in the same incubation solution, ensuring that all samples were subjected to the same conditions.

Figure 1

Capillary staining. Capillaries were visualized using lectin as described previously (Ballak et al., 2016). Briefly, air-dried sections were fixed with ice-cold acetone for 15 min, and blocked with 0.1% bovine serum albumin (BSA) diluted in 2-[4-(2-hydroxyethyl)piperazin-1-yl] ethanesulfonic acid (HEPES) for 60 min. Subsequently, the sections were treated with a peroxide solution for 30 min and incubated with biotinylated *Griffonia (Bandeira) simplicifolia* lectin (GSL I; Vector Laboratories, Peterborough, UK; 50 $\mu g \cdot mL^{-1}$ diluted in 1% BSA/HEPES) for 60 min. A 5-min wash with HEPES was conducted between each step. Sections were then

treated with avidin-biotinylated horseradish peroxidase (Vectastain ABCkit, Vector Laboratories) for 60 min, washed with HEPES, and incubated with Horse Radish Peroxidase Substrate Diaminobenzidine (Vectastain DAB kit, Vector Laboratories) for 5 min. After a wash in distilled water, the sections were mounted in glycerol gelatin (Sigma-Aldrich, UK). Characteristic staining of diaphragm in old mouse is shown in Figure 1.

Morphometry

Stained sections were photographed with a digital camera (Carl Zeiss) on a light microscope (Carl Zeiss, Germany). Two images per muscle cross-section were taken and 200 ± 85 (soleus, 186 ± 81; EDL, 194 ± 61; diaphragm, 216 ± 99) complete fibers were analyzed per sample.

Intramyocellular lipid. The IMCL content of individual fibers was determined using a microscope (Carl Zeiss, Germany) with a 20× objective and bright field settings. Images were digitally captured using a black and white AxioCam ICMI camera (Carl Zeiss) and analyzed with ImageJ (National Institutes of Health, USA, https://imagej.nih.gov/ij/). The fiber of interest was outlined, and the grey levels were converted to optical density (OD) using a calibration curve constructed from a series of filters of known OD. For each section, a separate calibration curve was constructed, and all images were taken at the same exposure with the same microscope settings. The OD of the Sudan Black B stain was determined in individual fibers and the background OD for each fiber was subtracted from the OD measured; the higher the OD for the Sudan Black B stain, the higher the IMCL content of the fiber.

Fiber type composition and fiber size. The fiber outlines and capillary centers were collected with a digitizing program (Btablet, BaLoH Software, Ooij, the Netherlands) and the data analyzed with AnaTis (BaLoH Software, http://www.baloh.nl). The fiber-type composition was expressed as number percentage. The fiber cross-sectional area (FCSA) was calculated for each fiber. An increased variation in fiber size may be an early hallmark of ageing, where small fibers might be atrophied as a consequence of denervation following motor neuron loss, and larger fibers may reflect compensatory hypertrophy. To investigate this, we also compared the standard deviation of the FCSA between the three muscles and the 20- and 79-week-old mice.

Succinate dehydrogenase. Photomicrographs of sections stained for SDH were taken on a light microscope with a 660-nm interference filter and a black and white AxioCam ICMI camera (Göttingen, Germany). All images were taken at the same exposure with the same microscope

settings. Images were analyzed using ImageJ (National Institutes of Health, USA). To measure the optical density (OD) of a given fiber, the outline of the fiber was drawn, and the background OD subtracted. For each session, a separate calibration curve was made with filters of known OD (A_{660}). The calibration curve was used to convert the absorbance values of the SDH staining into OD values. It has been shown in single muscle cells that the intensity of the staining is linearly related to the maximal oxygen consumption of the fiber (van der Laarse et al., 1989).

To assess the SDH activity (SDH-OD), the OD (A_{660}) was converted to the rate of staining and expressed as the increase in absorbance at 660 nm (A_{660}) per µm section thickness per second of incubation time ($\Delta A_{660} \cdot \mu m^{-1} \cdot s^{-1}$). The SDH-OD multiplied by the FCSA yielded the integrated SDH activity (SDH-INT in $\Delta A_{660} \cdot \mu m\ s^{-1}$):

$$\text{SDH-INT} = \text{SDH-OD X FCSA}$$

Capillarization. The capillarization in the muscles was determined with the method of capillary domains as described previously (Degens et al., 2006; Degens et al., 1992; Hoofd et al., 1985) with AnaTis. In short, a capillary domain is defined as the area of a muscle cross-section surrounding an individual capillary delineated by equidistant boundaries from adjacent capillaries. The capillary domain provides a good estimate of the capillary oxygen supply area, even in muscles with mixed fiber type composition (Al-Shammari et al., 2014). In addition to the overall parameters of muscle capillarization, including capillary density (CD; number of capillaries per mm^2) and the capillary to fiber ratio (C:F), this method allows to define the capillary supply to individual fibers even when they lack direct capillary contact. The local capillary to fiber ratio (LCFR), the sum of the fractions of the capillary domains overlapping a particular fiber, provides a continuous, rather than a discrete value of the capillary supply to a fiber and takes into consideration that a capillary supplies more than one fiber (Barnouin et al., 2017). The ratio of LCFR to the FCSA provides the capillary density for a given fiber, defined as the capillary fiber density (CFD).

The radius (R) of a domain, calculated from a circle with the same surface area, provides an indication of the maximal diffusion distance from the capillary to the edge of its domain. R shows a lognormal distribution, and thus the $Log_R SD$ (logarithmic standard deviation of the domain radius) is a measure of the heterogeneity of capillary spacing, where a larger value indicates a larger variability in the capillary domain sizes, and hence a less homogeneous distribution of the capillaries in the tissue. Model calculations have shown that increasing the

heterogeneity of capillary spacing results in poorer muscle oxygenation (Degens et al., 2006; Hoofd et al., 1985).

Statistical analysis

All statistical analyses were performed using IBM SPSS version 25. The Shapiro-Wilk test showed that all data were normally distributed. Where appropriate, a three-way (factors: age, muscle and fiber type) or two-way (factors: age and muscle) ANOVA was applied. Three-way interactions were excluded. If a main effect of age, muscle, fiber type or interactions was found, LSD post-hoc tests were performed to locate the differences. To assess the extent the capillary supply to a fiber was determined by the oxidative capacity of the fiber (SDH-OD), FCSA, fiber type, muscle of origin and/or age, a stepwise regression was performed. Statistical significance was accepted as $p < 0.05$. Data are expressed as mean±SD.

RESULTS

Table 1 **Mice characteristics**. The body mass was greater in 79- than 20-week-old mice ($p < 0.001$; Table 1), but the BMI was lower in 20- than 79-week-old mice ($p = 0.002$; Table 1). The mass of the soleus and EDL did not differ significantly between mice of different ages (Table 1). The MM/BM of the soleus and EDL were lower in 79- compared to 20-week-old mice ($p = 0.002$; Table 1).

Figure 2 **Muscle fiber type composition and fiber cross-sectional areas (Fig. 2)**.

Fiber type composition. Figure 2 shows the fiber type composition in the soleus (Fig. 2A), EDL (Fig. 2C) and diaphragm (Fig. 2E) in 20- and 79-week-old mice. The proportion of hybrid fibers was smaller than 5% in any of the muscles and hybrid fibers were therefore excluded from statistical analyses.

Type IIxb and type IIb fibers were only observed in the EDL. The proportion of type I fibers was higher in the soleus than in the diaphragm and EDL ($p < 0.001$), while for type IIx fibers the opposite was found ($p < 0.001$). The percentage of type IIa fibers was larger in the diaphragm than in the soleus and EDL ($p < 0.001$).

The proportion of type I, IIx and IIb fibers did not change significantly with age in any of the muscles. The muscle x age interaction ($p = 0.015$) for the type IIa fiber type proportion was reflected by a lower proportion of type IIa fibers in the soleus of 79- compared to 20- week-old mice ($p = 0.014$) and no significant age-related differences in the EDL and diaphragm.

Fiber cross-sectional area (FCSA). Figure 2B, D and F show the FCSA in soleus, EDL and diaphragm fibers, respectively. In the diaphragm and EDL type I and IIa fibers were smaller than type IIx and IIb fibers ($p \leq 0.002$), while in the soleus type I fibers were larger than type IIa and IIx fibers ($p \leq 0.032$).

The muscle x age interaction for FCSA ($p = 0.002$) was reflected by larger fibers in 79- than 20- week old mice in the diaphragm ($p < 0.001$), while in the EDL the opposite was found ($p = 0.001$). There was no significant effect of age on the FCSA in the soleus.

Variation in fiber size (SD FCSA) (Table 2). There was an effect of muscle on the SD FCSA ($p = 0.003$), but also a muscle * age interaction ($p = 0.044$; Table 2) that was reflected by a larger SD FCSA in the diaphragm than in the soleus and EDL in 20-week-old mice ($p < 0.001$), but no significant difference in SD FCSA between the muscles in the 79-week-old mice. The SD FCSA was larger in the EDL of 20- than 79-week-old mice ($p = 0.044$), with no significant age-related difference in the SD FCSA in the soleus and diaphragm.

Figure 3 **Intramyocellular lipid (IMCL) levels (Fig. 3)**

The IMCL content was higher in the diaphragm than in the soleus and EDL ($p < 0.001$), but there were no fiber type or ageing-related differences in IMCL levels in any of the muscles.

Figure 4 **Succinate dehydrogenase (SDH) activity (SDH-OD) (Fig. 4).**

The SDH-OD decreased in the following order: IIa>I,IIx>IIb ($p \leq 0.027$). The SDH-OD of fibers in the diaphragm was higher than that in the soleus and EDL ($p < 0.001$). The SDH-OD in muscle fibers did not differ significantly between 20- and 79-week-old animals.

The SDH-INT of muscle fibers was higher in the diaphragm and soleus than in the EDL ($p \leq 0.035$). While the SDH-INT was lower in the diaphragm of 20- than 79-week-old mice ($p = 0.046$), in the EDL the opposite was found ($p = 0.010$) with no significant age-related difference in the SDH-INT in the soleus.

Figure 5, 6 **Muscle capillarization (Fig. 5 & Fig. 6)**.

Table 2 *Indices of global capillary supply.* The C:F was soleus>diaphragm>EDL ($p \leq 0.002$) (Table 2). The C:F did not differ between age groups for any muscle. The CD was higher in the diaphragm than in the soleus and EDL ($p \leq 0.001$). The CD was lower in the diaphragm of 79- than 20-week-old mice ($p = 0.027$), while in the EDL the opposite was found ($p = 0.012$) with no significant age-related differences in the soleus.

The heterogeneity of capillary spacing, indicated by the $Log_R SD$ was EDL>soleus>diaphragm ($p \leq 0.043$) (Figure 5A). The $Log_R SD$ was higher in muscles of 20- than 79-week-old mice, irrespective of muscle ($p \leq 0.011$). The $Log_R SD$ in the muscles was positively corrected with the SD FCSA ($p = 0.030$; Figure 5B).

Local capillary to fiber ratio (LCFR). Figure 6 A, C and E show the LCFR. The LCFR of type I fibers was soleus>diaphragm>EDL ($p < 0.001$) and that of type IIa fibers was higher in the soleus than in the diaphragm and EDL ($p < 0.001$). The LCFR of type IIx fibers was larger in the diaphragm and soleus than in the EDL ($p < 0.034$). The LCFR of all fibers pooled was larger in the soleus than in the diaphragm and EDL ($p \leq 0.002$). Overall, there were no significant age-related differences in LCFR in any of the muscles.

Capillary fiber density (CFD). Figure 6 B, D and F show the CFD. Overall, the CFD of type IIb was smaller than that of type IIx, IIa and type I fibers ($p \leq 0.002$). There was a significant muscle x age interaction ($p < 0.001$). At 20 weeks of age, the CFD was larger in the diaphragm than in the soleus and EDL ($p < 0.001$). In the diaphragm, the CFD was lower in 79- than in 20-week-old mice ($p < 0.001$), while in the EDL the opposite was found ($p < 0.002$) with no significant difference in CFD in the soleus and EDL.

Figure 7, 8 **Determinants of fiber capillary supply (Fig. 7 & 8)**

To assess differences between muscles, fiber types and age in the matching of oxygen supply (LCFR) and demand (SDH-INT) of a fiber, the LCFR/SDH-INT was calculated as a measure of the supply:demand ratio. The LCFR/SDH-INT was higher in type IIb fibers in comparison to all other fiber types ($p<0.001$). There was a significant age x muscle interaction ($p = 0.001$), which was reflected by a higher LCFR/SDH-INT in the EDL of 79- than in 20-week-old mice ($p \leq 0.006$), while in the diaphragm the LCFR/SDH-INT the opposite was found ($p = 0.019$).

It appeared that the LCFR was primarily determined by FCSA (adjusted $R^2 = 0.550$; $p < 0.001$) and a small contribution of muscle of origin that increased the adjusted R^2 to 0.731 ($p < 0.001$) (Fig. 8). We also performed the analysis on all individual fibers ($n = 4663$), and this gave

essentially the same outcome: FCSA was the main determinant (adjusted $R^2 = 0.423$; $p < 0.001$), and muscle of origin increased the adjusted R^2 to 0.533 ($p < 0.001$). There were no significant contributions of age or SDH-OD, suggesting that the qualitative and quantitative relationships between size and oxidative capacity of fiber with capillary supply do not change during early ageing.

DISCUSSION

The main observations of the present study were that in mice, early ageing (between 20 and 79 weeks), characterized by an absence of a significant loss of hind limb muscle mass, was associated with hypertrophy in the diaphragm. This hypertrophy resulted in a reduction in the capillary supply to a fiber relative to oxidative capacity that was already lower in the diaphragm than the extensor digitorum longus (EDL) and soleus muscle. The capillary supply to a fiber relative to the oxidative capacity did increase in the EDL, indicative for a capillary supply in relative excess of oxidative capacity. These changes were almost entirely explicable by fiber hypertrophy in the diaphragm and fiber atrophy in the EDL, while no changes in morphology were seen in the soleus. Combined with previous observations in CD-1 mice these data indicate that in addition to a reduction in specific tension (Hill et al., 2018; Tallis et al., 2014) 1) diaphragm hypertrophy is a hallmark of early ageing, 2) fiber atrophy is not necessarily preceded by capillary rarefaction and reductions in oxidative capacity, and 3) different muscles undergo different patterns of ageing.

Morphological differences between muscles

In line with previous studies (Greising et al., 2013; Omairi et al., 2016), we found that, irrespective of age, the mouse soleus contains mostly type I and IIa fibers, whereas the EDL is predominantly composed of type IIb fibers and the diaphragm has primarily type IIa and type IIx fibers. Overall, the mouse soleus had the largest and the diaphragm the smallest fibers. Larger fibers in the soleus than the EDL have been observed previously in mice (Omairi et al., 2016). Irrespective of fiber type, the oxidative capacity of fibers was higher in diaphragm compared to those in the soleus and EDL, something also seen in rats (Smith et al., 1988). Part of the explanation of the higher oxidative capacity and IMCL content in fibers of the diaphragm may be that it is continuously active and comparable to a trained muscle that has higher IMCL stores and fatty acid oxidative capacity (van der Vusse and Reneman 1996). Whatever the

cause, these observations indicate that the properties of the fibers of a given type are dependent on the muscle of origin.

In agreement with a previous study on muscle capillarization (Murakami et al., 2010), we found that the capillary to fiber ratio (C:F) was higher in soleus compared with EDL and diaphragm. The CD was, however, highest in the diaphragm. The heterogeneity of capillary spacing, reflected by the logarithmic standard deviation of the capillary supply radius (Log_RSD) (Barnouin et al., 2017; Degens et al., 1993b; Hoofd et al., 1985) has a significant effect on tissue oxygenation (Degens et al., 2006; Degens et al., 1994; Goldman et al., 2006) and was in 20-week-old mice smaller in the diaphragm than the soleus and EDL, and may be related to the higher oxidative capacity of the diaphragm requiring a more homogeneous oxygen tension in this than the other two muscles.

Early ageing

In contrast to the average life expectancy of 26.7 months (115.7 weeks) of C57BL/6 mice (Ballak et al., 2014), the 50% survival of female CD-1 mice is 78-80 weeks (Navarro et al., 2002). However, it has been found that the specific tension and power output normalized to muscle mass of the EDL and diaphragm is lower in 30- and 50- than 10-week-old mice, but without significant differences in maximal tetanic force or muscle atrophy (Hill et al., 2018; Tallis et al., 2014). The absence of significant differences in the mass of the soleus and EDL from 20- and 79-week-old mice in our study suggests that the observed reductions in specific tension are early signs of muscle ageing.

With ageing, selective type II atrophy is common in both human (Barnouin et al., 2017; Lexell et al., 1988; McPhee et al., 2018) and mouse muscles (Brooks and Faulkner 1988). At first glance, the atrophy of the EDL muscle fibers without significant atrophy of fibers in the diaphragm and soleus between 20 and 79 weeks of age seems to support this idea. However, within the EDL atrophy was not limited to type IIb fibers, as type I and IIa fibers also atrophied. Furthermore, in the diaphragm, in contrast to Greising et al. (2013), we observed an increase in the size of type IIx fibers. The discrepancy may be due to the comparison of different age groups of rodents, where we compared 20- with 79-week-old mice and Greising et al. (2013) compared 20- with 100-week-old mice, suggesting that diaphragm hypertrophy during early ageing is followed by diaphragm atrophy at an advanced age. The initial hypertrophy of the diaphragm during ageing may be an adaptation to the increased cost of breathing as a

consequence of an ageing-related reduction in lung compliance (Sharma and Goodwin 2006). Although another explanation for the discrepancy might be the use of C57BL/6 x 129 mice by Greising et al. (2013), where we used CD-1 mice with a shorter life span (Navarro et al., 2002), one would expect more pronounced atrophy in the diaphragm of our mice. Overall, it appears that the increase in fiber size during ageing in the respiratory muscles is opposite to the decreases in fast limb muscles, and the changes in muscle morphology during early ageing are more related to functional demands on the muscle than fiber type composition.

The oxidative capacity of the fibers in the soleus and the diaphragm did not change between 20 and 79 weeks. In the EDL muscle, the age-related decrease of the integrated SDH activity per fiber is explicable by both a reduction (though not significant) in the mass-specific oxidative capacity (SDH-OD) and fiber cross-sectional area. The increase in fiber size in the diaphragm during early ageing was not accompanied by an increase in mitochondria, as indicated by the similar integrated SDH, a measure of the total number of mitochondria in a cell.

It has been found previously in mice of similar ages that during early ageing the specific tension and power normalized to muscle mass of the EDL and soleus was reduced (Hill et al., 2018). In older obese mice there was a reduction in specific tension and power of the diaphragm (Hill et al., 2019), something also reported for the vastus lateralis muscle in older obese adults where this was associated with intramyocellular fat accumulation (Choi et al., 2016). We found, however, no age-related increase in IMCL content in any of the three muscles, corresponding with their largely unchanged oxidative capacity.

It has been suggested that capillary loss may precede the age-related fiber atrophy (Larsson et al., 2019). However, the absence of an age-related difference in C:F in any of the muscles, as also reported by others in humans (Snijders et al., 2017), suggests this is not the case, and in the EDL the CD was even increased during early ageing. This increased CD in the EDL was explicable by a decrease in the FCSA, while in the diaphragm the reduced CD was attributable to an increase in FCSA during early ageing, without any indications of angiogenesis or capillary rarefaction, respectively.

In contrast to previous observations in rats (Degens et al., 2009), we found that the heterogeneity of capillary spacing did, if anything, decrease during early ageing, suggesting a more homogeneous distribution of capillaries. It should be noted, however, that the increased heterogeneity occurred in rats that were at a relatively more advanced age than our oldest mice,

and was associated with an increased variation in fiber sizes in the muscle (Degens et al., 2009). While here we also showed that the heterogeneity of capillary spacing increased with an increase in the variation in fiber size (Fig. 5B), there was no significant change in the variation in fiber size during early ageing in the muscles of our mice. Overall, this corresponds with the suggestion that 1) the constraint of capillary positioning at the periphery of a fiber is one determinant of the heterogeneity of capillary spacing (Degens et al., 2009), and 2) that the location of capillaries is not random but controlled (Degens et al., 2006), at least up to early ageing, to maintain sufficient muscle oxygenation.

These data indicate that the ageing-related changes in muscle morphology differ markedly between muscles; there is fiber hypertrophy (~30%) in the diaphragm and fiber atrophy (~30%) in the EDL. Such changes during early ageing may be masked if the young control group has not yet fully developed muscles and this emphasizes the importance of selecting appropriate age groups when using rodent models to study (early pre-sarcopenic) muscle ageing (Ballak et al., 2014).

Determinants of fiber capillary supply

In line with others (Barnouin et al., 2017; Bosutti et al., 2015; Degens et al., 1992), we found that the main determinant of the number of capillaries supplying a fiber (LCFR) was fiber size. This relationship differed somewhat between muscles, as reflected by the higher CFD in the diaphragm than the soleus and EDL, suggesting that the relationship between fiber size and capillary supply to a fiber is somewhat modulated by the metabolic surrounding of the fiber. In contrast to common assumptions, we have previously reported that the capillary supply to a fiber is not determined by the oxidative capacity of the fiber itself (Barnouin et al., 2017; Bosutti et al., 2015). Similarly, in the present study, the oxidative capacity did not significantly contribute to the capillary supply of a fiber. To investigate the relationship between supply and demand further we estimated the maximal oxygen demand of a fiber as the integrated SDH activity (FCSA * SDH-OD) and calculated the capillary supply (LCFR) to demand ratio (LCFR/SDH-INT) for each fiber. In contrast to expectations, the diaphragm had the lowest and the EDL the highest supply to demand ratio. Similar to hypertrophied hearts (Des Tombe et al., 2002), the lower supply to demand ratio in the diaphragm may indicate that oxygen supply may be at risk of being compromised in maximally working diaphragm, and less so in soleus and EDL muscles, which becomes even more compromised during ageing, as reflected by the lower ratio in the diaphragm of 79- than 20-week-old mice. On the other hand, the higher supply to

demand ratio in the EDL than in the soleus and diaphragm suggests that there is an excessive capillary supply in the EDL in relation to its oxidative capacity.

During early ageing, the capillary supply to demand ratio increased in the soleus, but not in the diaphragm, suggesting that, as seen in ageing rat muscle (Hepple and Vogell 2004), the capillary supply becomes even more in excess to oxidative capacity, particularly in the soleus muscle. This again supports the notion that the oxidative capacity is not the main determinant of the capillary supply to a fiber, but other functions, such as removal of heat and waste products, and substrate delivery are more important. It is even possible that the capillary supply limits for these reasons fiber size, rather than fiber size determining the capillary supply (Hendrickse and Degens 2019; Larsson et al., 2019).

Conclusion

The current study showed that in mouse muscles during early ageing, characterized by an absence of significant loss of muscle mass in the hind limb muscles, the EDL fibers had atrophied, and interestingly, the diaphragm hypertrophied without changes in the number of capillaries supplying a fiber or their oxidative capacity. It, therefore, appears that early ageing exerts differing effects in respiratory and limb muscles, where atrophy is not necessarily accompanied with, or preceded by, capillary rarefaction. Nevertheless, at any age and in all muscles the fiber size was the main determinant of capillary supply to a fiber, with no significant contribution of oxidative capacity.

Disclosure The authors declare no conflict of interest.

REFERENCES

Ahmed, S.K.; Egginton, S.; Jakeman, P.M.; Mannion, A.F.; Ross, H.F. Is human skeletal muscle capillary supply modelled according to fibre size or fibre type? Exp Physiol. 82:231-234; 1997

Al-Shammari, A.A.; Gaffney, E.A.; Egginton, S. Modelling capillary oxygen supply capacity in mixed muscles: Capillary domains revisited. J Theor Biol. 356:47-61; 2014

Aldinger, K.A.; Sokoloff, G.; Rosenberg, D.M.; Palmer, A.A.; Millen, K.J. Genetic Variation and Population Substructure in Outbred CD-1 Mice: Implications for Genome-Wide Association Studies. Plos One. 4; 2009

Allman, B.L.; Rice, C.L. Neuromuscular fatigue and aging: central and peripheral factors. Muscle Nerve. 25:785-796; 2002

Andersen, J.L. Muscle fibre type adaptation in the elderly human muscle. Scand J Med Sci Spor. 13:40-47; 2003

Ballak, S.B.; Buse-Pot, T.; Harding, P.J.; Yap, M.H.; Deldicque, L.; de Haan, A.; Jaspers, R.T.; Degens, H. Blunted angiogenesis and hypertrophy are associated with increased fatigue resistance and unchanged aerobic capacity in old overloaded mouse muscle. Age (Dordr). 38:39; 2016

Ballak, S.B.; Degens, H.; de Haan, A.; Jaspers, R.T. Aging related changes in determinants of muscle force generating capacity: a comparison of muscle aging in men and male rodents. Ageing Res Rev. 14:43-55; 2014

Barnouin, Y.; McPhee, J.S.; Butler-Browne, G.; Bosutti, A.; De Vito, G.; Jones, D.A.; Narici, M.; Behin, A.; Hogrel, J.Y.; Degens, H. Coupling between skeletal muscle fiber size and capillarization is maintained during healthy aging. J Cachexia Sarcopenia Muscle; 2017

Bosutti, A.; Egginton, S.; Barnouin, Y.; Ganse, B.; Rittweger, J.; Degens, H. Local capillary supply in muscle is not determined by local oxidative capacity. J Exp Biol. 218:3377-3380; 2015

Brooks, S.V.; Faulkner, J.A. Contractile Properties of Skeletal-Muscles from Young, Adult and Aged Mice. J Physiol-London. 404:71-82; 1988

Callahan, D.M.; Kent-Braun, J.A. Effect of old age on human skeletal muscle force-velocity and fatigue properties. J Appl Physiol. 111:1345-1352; 2011

Chan, S.; Head, S.I. Age- and Gender-Related Changes in Contractile Properties of Non-Atrophied EDL Muscle. Plos One. 5; 2010

Choi, S.J.; Files, D.C.; Zhang, T.; Wang, Z.M.; Messi, M.L.; Gregory, H.; Stone, J.; Lyles, M.F.; Dhar, S.; Marsh, A.P.; Nicklas, B.J.; Delbono, O. Intramyocellular Lipid and Impaired Myofiber Contraction in Normal Weight and Obese Older Adults. J Gerontol a-Biol. 71:557-564; 2016

Degens, H.; Alway, S.E. Control of muscle size during disuse, disease, and aging. International Journal of Sports Medicine. 27:94-99; 2006

Degens, H.; Deveci, D.; Botto-Van Bemden, A.; Hoofd, L.J.C.; Egginton, S. Maintenance of heterogeneity of capillary spacing is essential for adequate oxygenation in the soleus muscle of the growing rat. Microcirculation. 13:467-476; 2006

Degens, H.; Korhonen, M.T. Factors contributing to the variability in muscle ageing. Maturitas. 73:197-201; 2012

Degens, H.; Morse, C.I.; Hopman, M.T. Heterogeneity of capillary spacing in the hypertrophied plantaris muscle from young-adult and old rats. Adv Exp Med Biol. 645:61-66; 2009

Degens, H.; Ringnalda, B.E.M.; Hoofd, L.J.C. Capillarisation, Fibre Types and Myoglobin Content of the Dog Gracilis Muscle. Oxygen Transport to Tissue Xvi. 361:533-539; 1994

Degens, H.; Turek, Z.; Binkhorst, R.A. Compensatory Hypertrophy and Training Effects on the Functioning of Aging Rat M-Plantaris. Mechanisms of Ageing and Development. 66:299-311; 1993a

Degens, H.; Turek, Z.; Hoofd, L.; Vanthof, M.A.; Binkhorst, R.A. Capillarization and Fiber Types in Hypertrophied M-Plantaris in Rats of Various Ages. Resp Physiol. 94:217-226; 1993b

Degens, H.; Turek, Z.; Hoofd, L.J.C.; Vanthof, M.A.; Binkhorst, R.A. The Relationship between Capillarization and Fiber Types during Compensatory Hypertrophy of the Plantaris Muscle in the Rat. J Anat. 180:455-463; 1992

Degens, H.; Veerkamp, J.H. Changes in Oxidative Capacity and Fatigue Resistance in Skeletal-Muscle. Int J Biochem. 26:871-878; 1994

Delmonico, M.J.; Harris, T.B.; Visser, M.; Park, S.W.; Conroy, M.B.; Velasquez-Mieyer, P.; Boudreau, R.; Manini, T.M.; Nevitt, M.; Newman, A.B.; Goodpaster, B.H.; Health, A.;

Body. Longitudinal study of muscle strength, quality, and adipose tissue infiltration. Am J Clin Nutr. 90:1579-1585; 2009
Des Tombe, A.L.; Van Beek-Harmsen, B.J.; Lee-De Groot, M.B.; Van Der Laarse, W.J. Calibrated histochemistry applied to oxygen supply and demand in hypertrophied rat myocardium. Microsc Res Tech. 58:412-420; 2002
Egginton, S.; Badr, I.; Williams, J.; Hauton, D.; Baan, G.C.; Jaspers, R.T. Physiological angiogenesis is a graded, not threshold, response. J Physiol-London. 589:195-206; 2011
Egginton, S.; Turek, Z.; Hoofd, L.J.C. Differing Patterns of Capillary Distribution in Fish and Mammalian Skeletal-Muscle. Resp Physiol. 74:383-396; 1988
Fragala, M.S.; Kenny, A.M.; Kuchel, G.A. Muscle quality in aging: a multi-dimensional approach to muscle functioning with applications for treatment. Sports Med. 45:641-658; 2015
Goldman, D.; Bateman, R.M.; Ellis, C.G. Effect of decreased O2 supply on skeletal muscle oxygenation and O2 consumption during sepsis: role of heterogeneous capillary spacing and blood flow. Am J Physiol Heart Circ Physiol. 290:H2277-2285; 2006
Green, H.; Goreham, C.; Ouyang, J.; Ball-Burnett, M.; Ranney, D. Regulation of fiber size, oxidative potential, and capillarization in human muscle by resistance exercise. Am J Physiol. 276:R591-596; 1999
Greising, S.M.; Mantilla, C.B.; Gorman, B.A.; Ermilov, L.G.; Sieck, G.C. Diaphragm muscle sarcopenia in aging mice. Exp Gerontol. 48:881-887; 2013
Hendrickse, P.; Degens, H. The role of the microcirculation in muscle function and plasticity. J Muscle Res Cell Motil; 2019
Hepple, R.T.; Vogell, J.E. Anatomic capillarization is maintained in relative excess of fiber oxidative capacity in some skeletal muscles of late middle-aged rats. J Appl Physiol. 96:2257-2264; 2004
Hill, C.; James, R.S.; Cox, V.M.; Tallis, J. The Effect of Increasing Age on the Concentric and Eccentric Contractile Properties of Isolated Mouse Soleus and Extensor Digitorum Longus Muscles. J Gerontol A Biol Sci Med Sci. 73:579-587; 2018
Hill, C.; James, R.S.; Cox, V.M.; Tallis, J. Does Dietary-Induced Obesity in Old Age Impair the Contractile Performance of Isolated Mouse Soleus, Extensor Digitorum Longus and Diaphragm Skeletal Muscles? Nutrients. 11; 2019
Hogrel, J.Y.; Barnouin, Y.; Azzabou, N.; Butler-Browne, G.; Voit, T.; Moraux, A.; Leroux, G.; Behin, A.; McPhee, J.S.; Carlier, P.G. NMR imaging estimates of muscle volume and intramuscular fat infiltration in the thigh: variations with muscle, gender, and age. Age (Dordr). 37:9798; 2015
Holloway, T.M.; Snijders, T.; Van Kranenburg, J.; Van Loon, L.J.C.; Verdijk, L.B. Temporal Response of Angiogenesis and Hypertrophy to Resistance Training in Young Men. Med Sci Sport Exer. 50:36-45; 2018
Hoofd, L.; Turek, Z.; Kubat, K.; Ringnalda, B.E.M.; Kazda, S. Variability of Intercapillary Distance Estimated on Histological Sections of Rat-Heart. Advances in Experimental Medicine and Biology. 191:239-247; 1985
Klitgaard, H.; Zhou, M.; Schiaffino, S.; Betto, R.; Salviati, G.; Saltin, B. Aging Alters the Myosin Heavy-Chain Composition of Single Fibers from Human Skeletal-Muscle. Acta Physiol Scand. 140:55-62; 1990
Kob, R.; Bollheimer, L.C.; Bertsch, T.; Fellner, C.; Djukic, M.; Sieber, C.C.; Fischer, B.E. Sarcopenic obesity: molecular clues to a better understanding of its pathogenesis? Biogerontology. 16:15-29; 2015
Komiya, Y.; Sawano, S.; Mashima, D.; Ichitsubo, R.; Nakamura, M.; Tatsumi, R.; Ikeuchi, Y.; Mizunoya, W. Mouse soleus (slow) muscle shows greater intramyocellular lipid droplet

accumulation than EDL (fast) muscle: fiber type-specific analysis. J Muscle Res Cell M. 38:163-173; 2017

Larsson, L.; Degens, H.; Li, M.; Salviati, L.; Lee, Y.I.; Thompson, W.; Kirkland, J.L.; Sandri, M. Sarcopenia: Aging-Related Loss of Muscle Mass and Function. Physiol Rev. 99:427-511; 2019

Lexell, J.; Taylor, C.C.; Sjostrom, M. What is the cause of the ageing atrophy? Total number, size and proportion of different fiber types studied in whole vastus lateralis muscle from 15- to 83-year-old men. J Neurol Sci. 84:275-294; 1988

McPhee, J.S.; Cameron, J.; Maden-Wilkinson, T.; Piasecki, M.; Yap, M.H.; Jones, D.A.; Degens, H. The Contributions of Fiber Atrophy, Fiber Loss, In Situ Specific Force, and Voluntary Activation to Weakness in Sarcopenia. J Gerontol a-Biol. 73:1287-1294; 2018

McPhee, J.S.; French, D.P.; Jackson, D.; Nazroo, J.; Pendleton, N.; Degens, H. Physical activity in older age: perspectives for healthy ageing and frailty. Biogerontology. 17:567-580; 2016

Murakami, S.; Fujino, H.; Takeda, I.; Momota, R.; Kumagishi, K.; Ohtsuka, A. Comparison of Capillary Architecture between Slow and Fast Muscles in Rats Using a Confocal Laser Scanning Microscope. Acta Med Okayama. 64:11-18; 2010

Navarro, A.; Sanchez Del Pino, M.J.; Gomez, C.; Peralta, J.L.; Boveris, A. Behavioral dysfunction, brain oxidative stress, and impaired mitochondrial electron transfer in aging mice. Am J Physiol Regul Integr Comp Physiol. 282:R985-992; 2002

Omairi, S.; Matsakas, A.; Degens, H.; Kretz, O.; Hansson, K.A.; Solbra, A.V.; Bruusgaard, J.C.; Joch, B.; Sartori, R.; Giallourou, N.; Mitchell, R.; Collins-Hooper, H.; Foster, K.; Pasternack, A.; Ritvos, O.; Sandri, M.; Narkar, V.; Swann, J.R.; Huber, T.B.; Patel, K. Enhanced exercise and regenerative capacity in a mouse model that violates size constraints of oxidative muscle fibres. Elife. 5; 2016

Plyley, M.J.; Olmstead, B.J.; Noble, E.G. Time course of changes in capillarization in hypertrophied rat plantaris muscle. J Appl Physiol. 84:902-907; 1998

Polkey, M.I.; Harris, M.L.; Hughes, P.D.; Hamnegard, C.H.; Lyons, D.; Green, M.; Moxham, J. The contractile properties of the elderly human diaphragm. Am J Resp Crit Care. 155:1560-1564; 1997

Rahemi, H.; Nigam, N.; Wakeling, J.M. The effect of intramuscular fat on skeletal muscle mechanics: implications for the elderly and obese. J R Soc Interface. 12; 2015

Rice, M.C.; Obrien, S.J. Genetic Variance of Laboratory Outbred Swiss Mice. Nature. 283:157-161; 1980

Schwenzer, N.F.; Martirosian, P.; Machann, J.; Schraml, C.; Steidle, G.; Claussen, C.D.; Schick, F. Aging Effects on Human Calf Muscle Properties Assessed by MRI at 3 Tesla. J Magn Reson Imaging. 29:1346-1354; 2009

Sharma, G.; Goodwin, J. Effect of aging on respiratory system physiology and immunology. Clin Interv Aging. 1:253-260; 2006

Sjogren, K.; Hellberg, N.; Bohlooly-Y, M.; Savendahl, L.; Johansson, M.S.; Berglindh, T.; Bosaeus, I.; Ohlsson, C. Body fat content can be predicted in vivo in mice using a modified dual-energy X-ray absorptiometry technique. J Nutr. 131:2963-2966; 2001

Smith, D.; Green, H.; Thomson, J.; Sharratt, M. Oxidative potential in developing rat diaphragm, EDL, and soleus muscle fibers. Am J Physiol. 254:C661-668; 1988

Snijders, T.; Nederveen, J.P.; Joanisse, S.; Leenders, M.; Verdijk, L.B.; van Loon, L.J.C.; Parise, G. Muscle fibre capillarization is a critical factor in muscle fibre hypertrophy during resistance exercise training in older men. J Cachexia Sarcopeni. 8:267-276; 2017

Tallis, J.; Hill, C.; James, R.S.; Cox, V.M.; Seebacher, F. The effect of obesity on the contractile performance of isolated mouse soleus, EDL, and diaphragm muscles. J Appl Physiol (1985). 122:170-181; 2017

Tallis, J.; James, R.S.; Little, A.G.; Cox, V.M.; Duncan, M.J.; Seebacher, F. Early effects of ageing on the mechanical performance of isolated locomotory (EDL) and respiratory (diaphragm) skeletal muscle using the work-loop technique. Am J Physiol-Reg I. 307:R670-R684; 2014

Teramoto, S.; Fukuchi, Y.; Nagase, T.; Matsuse, T.; Orimo, H. A Comparison of Ventilation Components in Young and Elderly Men during Exercise. J Gerontol a-Biol. 50:B34-B39; 1995

Tolep, K.; Higgins, N.; Muza, S.; Criner, G.; Kelsen, S.G. Comparison of Diaphragm Strength between Healthy Adult Elderly and Young Men. Am J Resp Crit Care. 152:677-682; 1995

van der Laarse, W.J.; Diegenbach, P.C.; Elzinga, G. Maximum rate of oxygen consumption and quantitative histochemistry of succinate dehydrogenase in single muscle fibres of Xenopus laevis. J Muscle Res Cell Motil. 10:221-228; 1989

van der Vusse, G.J.; Reneman, R.S. Lipid metabolism in muscle. in: Rowell L.B., Shepherd J.T., eds. Handbook of Physiology. New york: Oxford University Press; 1996

Wust, R.C.; Gibbings, S.L.; Degens, H. Fiber capillary supply related to fiber size and oxidative capacity in human and rat skeletal muscle. Adv Exp Med Biol. 645:75-80; 2009

Young, A.; Stokes, M.; Crowe, M. The size and strength of the quadriceps muscles of old and young men. Clin Physiol. 5:145-154; 1985

Table 1. Body and muscle mass in 20- and 79-week-old female CD-1 mice.

	20 weeks (n = 29)	79 weeks (n = 30)
BM (g)	38.5 (4.9)	47.2 (8.6)[1]
BMI ($kg \cdot m^{-2}$)	3.04 (0.34)	3.37 (0.41)[1]
Soleus (mg)	10.1 (1.6) (n =10)	9.4 (1.4) (n =10)
Soleus MM/BM ($mg \cdot g^{-1}$)	0.26 (0.04) (n =10)	0.20 (0.04)[1] (n =10)
EDL (mg)	10.0 (2.1) (n =10)	10.6 (1.8) (n =10)
EDL MM/BM ($mg \cdot g^{-1}$)	0.28 (0.06) (n =10)	0.24 (0.05)[1] (n =10)

BM: Body mass; BMI: body mass index (body mass divided by snout-to-anus length squared); EDL: extensor digitorum longus muscle; MM/BM: muscle mass divided by BM. [1] different from 20 weeks at $p \leq 0.002$. Data are mean ± SD.

Table 2. Indices of capillary supply in mouse soleus, extensor digitorum longus (EDL) and diaphragm

	Soleus		EDL		Diaphragm		Effect (p-values)		Interaction (p values)
	20w (n = 6)	79w (n = 5)	20w (n =3)	79w (n = 3)	20w (n = 7)	79w (n = 5)	Age	Muscle	A x M
C:F ratio	2.89[d,e] (0.20)	2.89 [e] (0.59)	1.80[s,d] (0.29)	1.73[s] (0.23)	2.45[s,e] (0.32)	2.31 (0.37)	0.633	< 0.001	0.966
CD (mm^{-2})	951[d] (106)	1066 (220)	625[d] (65)	1193[1] (213)	1659[s,e] (322)	1245[1] (173)	0.302	< 0.001	0.001
SD FCSA pooled	814[d] (146)	977 (404)	965[d] (132)	572[1] (194)	443[s,e] (104)	612 (246)	0.821	0.003	0.044

A x M, age × muscle interaction; Inter., interaction; w = weeks; CD, numerical capillary density; C:F ratio, ratio between the number of capillaries and number of fibers; values between brackets indicate standard deviation; FCSA, fiber cross-sectional area. Data are presented as mean ± SD. [s] different from soleus at $p \leq 0.002$; [d] different from diaphragm at $p < 0.001$; [e] different from EDL at $p \leq 0.001$; [1] different from 20 weeks at $p < 0.05$.

FIGURE LEGENDS

Figure 1. Serial sections of diaphragm from a 79-week-old mouse stained for (**A**) intramyocellular fat, (**B**) myosin heavy chain (MHC), (**C**) capillaries and (**D**) succinate dehydrogenase (SDH) activity. Note that type IIa fibers (green) had a higher SDH activity than type I (blue) and type IIx (red) fibers. *: indicates same fiber in the four panels. Arrows indicate examples of capillaries. Scale bar = 100 µm.

Figure 2. Fiber type composition (A, C and E) and fiber cross-sectional area (FCSA) (B, D and F) in the **(A-B)** soleus, **(C-D)** extensor digitorum longus (EDL) and **(E-F)** diaphragm muscles of 20- and 79-week-old mice. Values are means ± SD (n = 3-7). ^{s} different from soleus; ^{d} different from diaphragm; ^{e} different from EDL at $p < 0.001$; ^{i} different from type I fibers at $p \leq 0.032$; ^{a} different from type IIa at $p \leq 0.002$; ^{1} different from 20 weeks at $p \leq 0.014$.

Figure 3. Intramyocellular lipid levels in the **A)** soleus, **B)** extensor digitorum longus (EDL) and **C)** diaphragm muscles of 20- and 79-week-old mice. Values are means ± SD (n = 3-7). ^{s} different from soleus; ^{d} different from diaphragm; ^{e} different from EDL at $p < 0.001$.

Figure 4. Succinate dehydrogenase (SDH) optical density (A, C and E) and integrated succinate dehydrogenase activity (SDH-INT) (B, D and F) in the **(A-B)** soleus, **(C-D)** extensor digitorum longus (EDL) and **(E-F)** diaphragm muscles of 20- and 79- week-old mice. Values are means ± SD (n = 3-7). ^{s} different from soleus; ^{d} different from diaphragm; ^{e} different from EDL at $p \leq 0.035$; ^{i} different from type I fibers at $p \leq 0.027$; ^{a} different from type IIa at $p < 0.001$; ^{x} different from type IIx fibers at $p < 0.001$; ^{1} different from 20 weeks at $p < 0.046$.

Figure 5. Heterogeneity of capillary spacing (Log_RSD) (A) and relationship between Log_RSD variation in fiber size (SD FCSA) (B) in the soleus, extensor digitorum longus (EDL) and diaphragm muscles of 20- and 79-week-old mice. Values are means ± SD (n = 3-7). ^{s} different from soleus at $p \leq 0.043$; ^{d} different from diaphragm at $p \leq 0.043$; ^{e} different from EDL at $p < 0.001$. ^{1} different from 20 weeks at $p \leq 0.011$.

Figure 6. Local capillary to fiber ratio (LCFR) (A, C and E) and capillary fiber density (CFD) (B, D and F) in the **(A-B)** soleus, **(C-D)** extensor digitorum longus (EDL) and **(E-F)** diaphragm muscles of 20- and 79-week-old mice. Values are means ± SD (n = 3-7). ^{s} different from soleus; ^{d} different from diaphragm; ^{e} different from EDL at $p \leq 0.002$; ^{i} different from type I fibers; ^{a} different from type IIa; ^{x} different from type IIx fibers; ^{b} different from type IIb fibers at $p \leq 0.036$; ^{l} different from 20 weeks at $p \leq 0.002$.

Figure 7. Local capillary to fiber ratio (LCFR):integrated succinate dehydrogenase activity (SDH-INT) in the **(A)** soleus, **(B)** extensor digitorum longus (EDL) and **(C)** diaphragm muscles of 20- and 79-week-old mice. Values are means ± SD (n = 3-7). ^{s} different from soleus; ^{d} different from diaphragm; ^{e} different from EDL at $p \leq 0.022$; ^{i} different from type I fibers; ^{a} different from type IIa; ^{x} different from type IIx at $p < 0.001$; ^{l} different from 20 weeks at $p < 0.02$.

Figure 8. Relationship between the local capillary-to-fiber ratio (LCFR) and the fiber cross-sectional area (FCSA) in from soleus **(A)**, EDL **(B)** and diaphragm **(C)** muscles of 20- and 79-week-old mice. The FCSA and the LCFR was significantly correlated (soleus, n = 1663; EDL, n = 981; diaphragm, n = 2015). Each data point comes from an individual fiber.

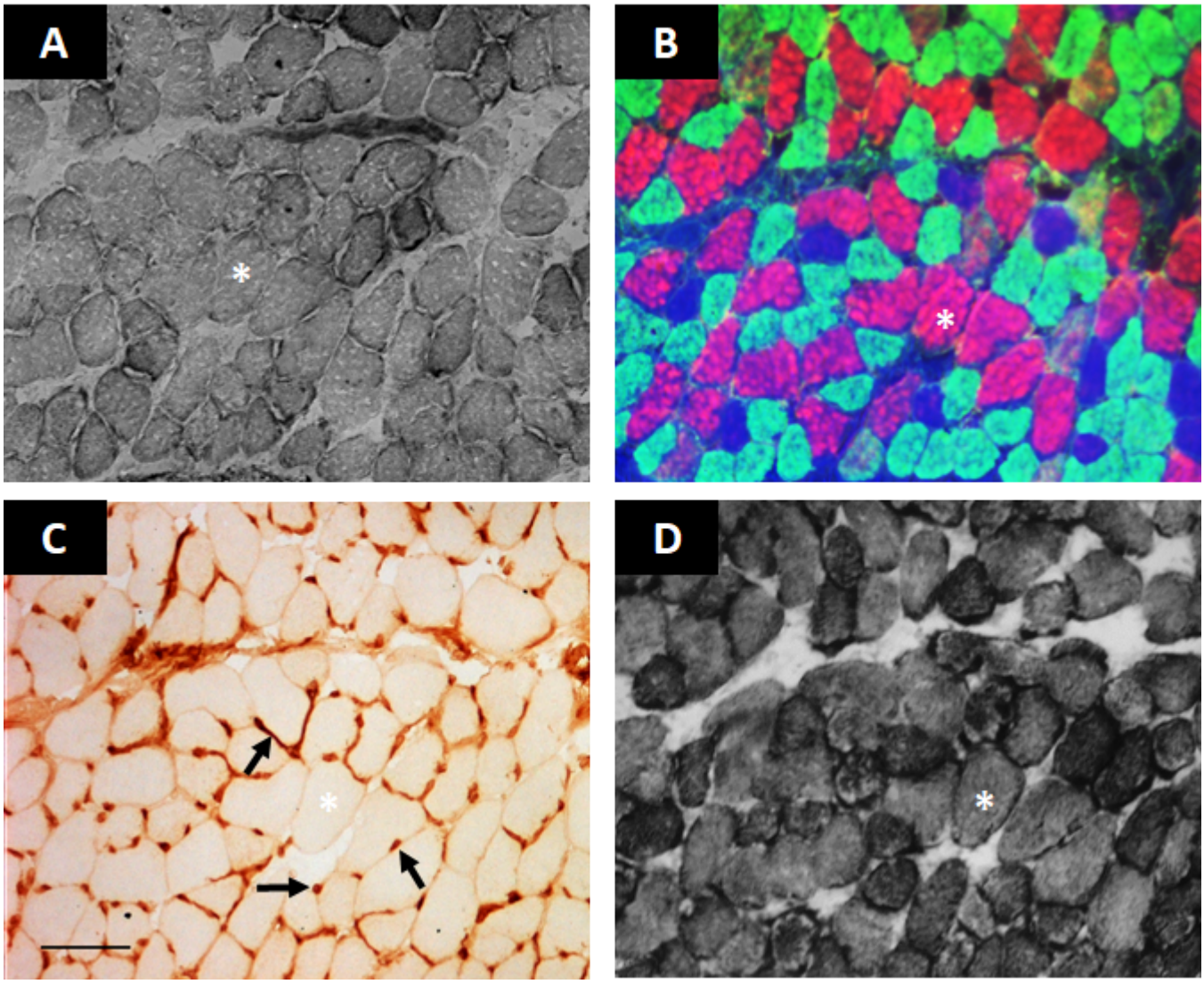
A
B
C
D

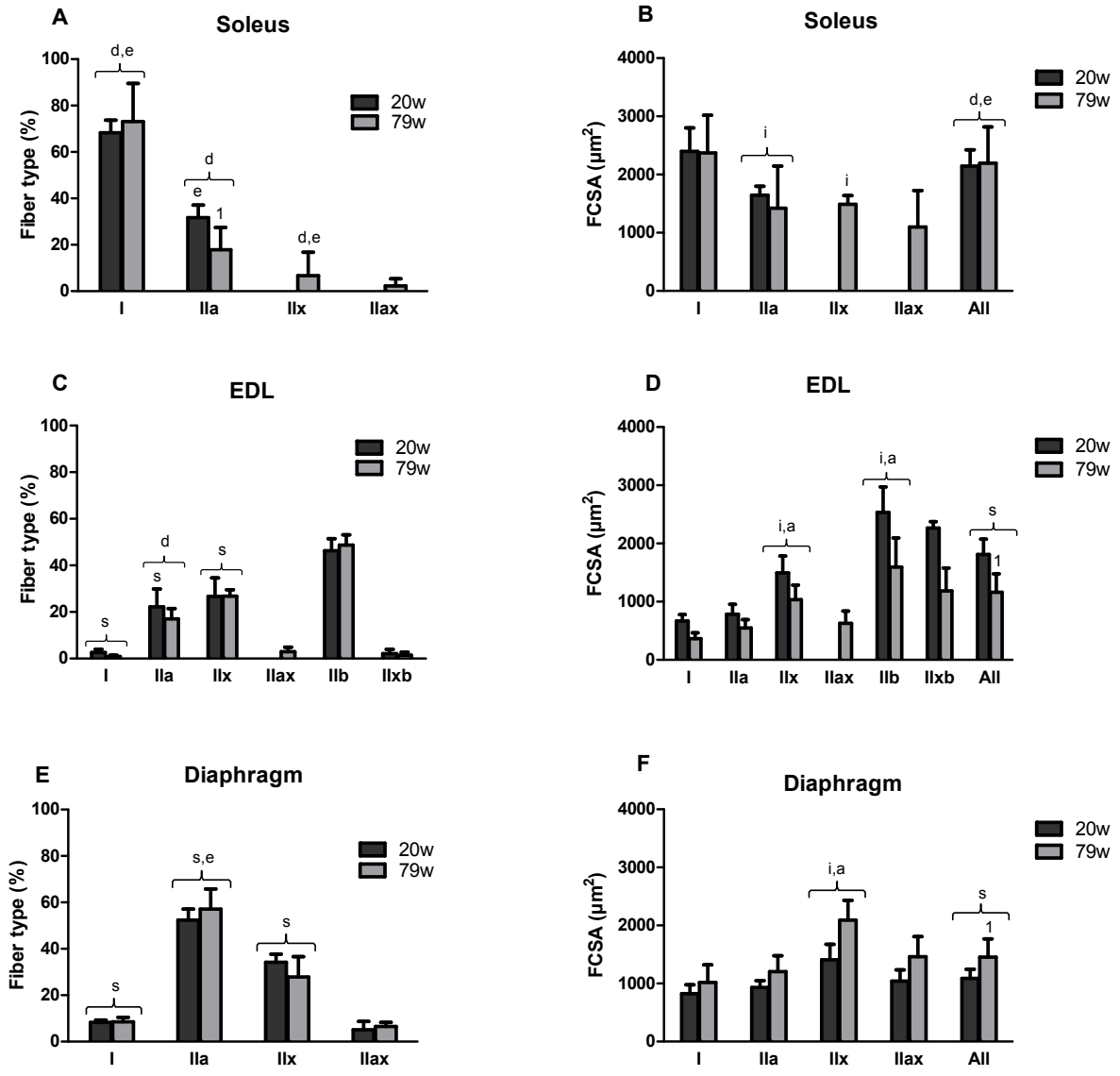
A
Soleus
Fiber type (%)
20w
79w
I
IIa
IIx
IIax
B
Soleus
FCSA (µm²)
All
C
EDL
IIb
IIxb
D
EDL
E
Diaphragm
F
Diaphragm

Figure 2

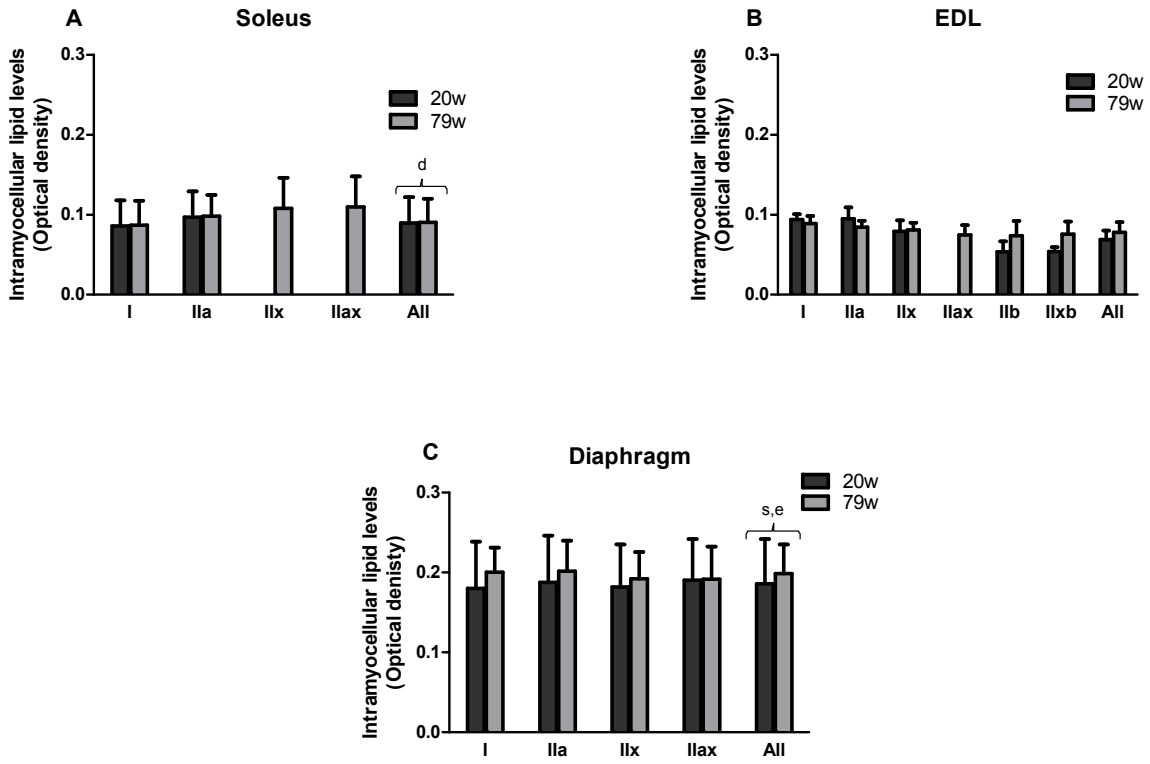
A
Soleus
Intramyocellular lipid levels (Optical density)
0.3
0.2
0.1
0.0
20w
79w
d
I
IIa
IIx
IIax
AII
B
EDL
Intramyocellular lipid levels (Optical density)
20w
79w
I
IIa
IIx
IIax
IIb
IIxb
AII
C
Diaphragm
Intramyocellular lipid levels (Optical denisty)
20w
79w
s,e
I
IIa
IIx
IIax
AII

Figure 3

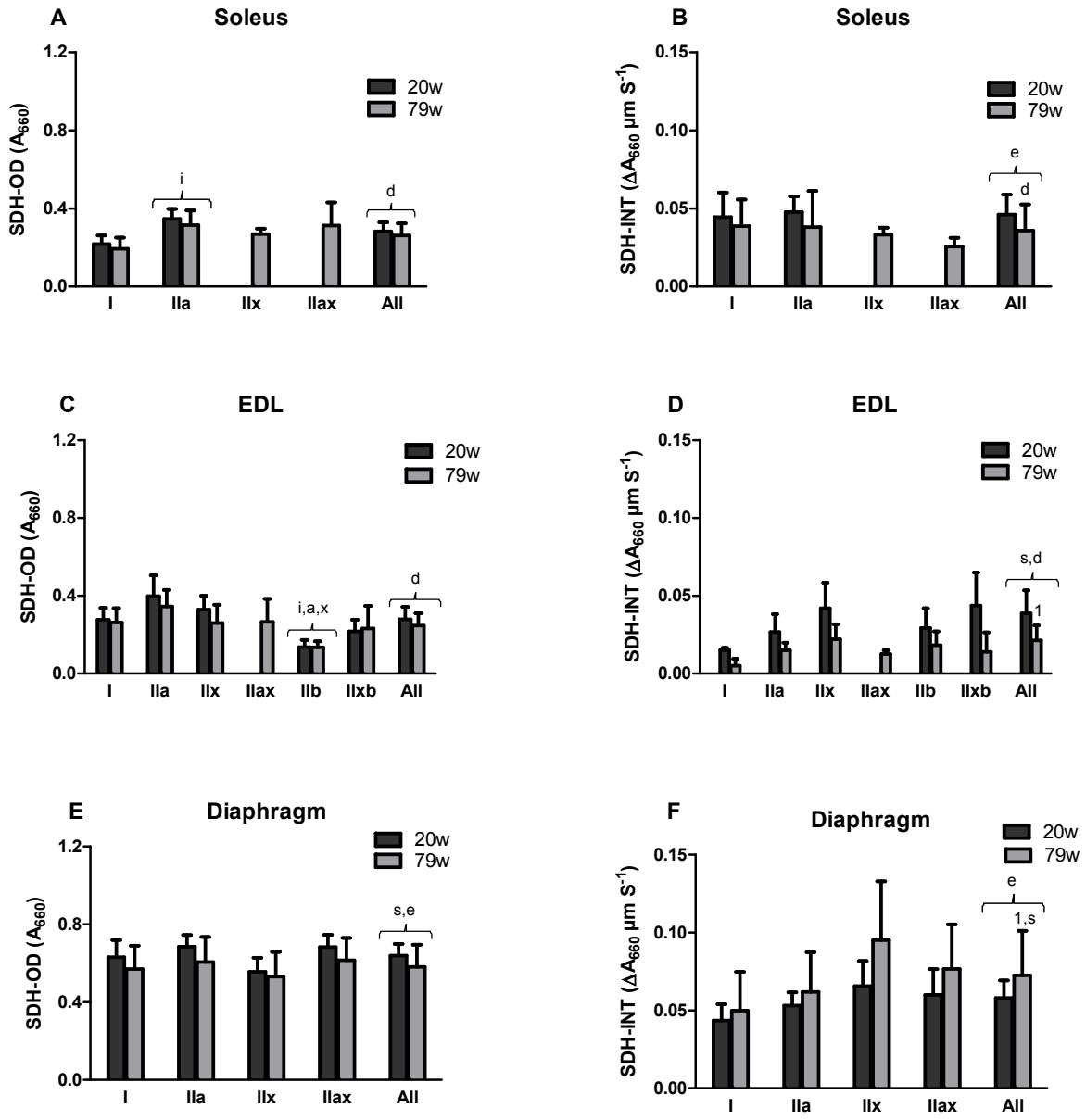
A
Soleus
SDH-OD (A660)
20w
79w
i
d
I
IIa
IIx
IIax
AII
B
Soleus
SDH-INT (ΔA660 µm s-1)
e
d
C
EDL
i,a,x
IIb
IIxb
D
EDL
s,d
1
E
Diaphragm
s,e
F
Diaphragm
1,s

Figure 4

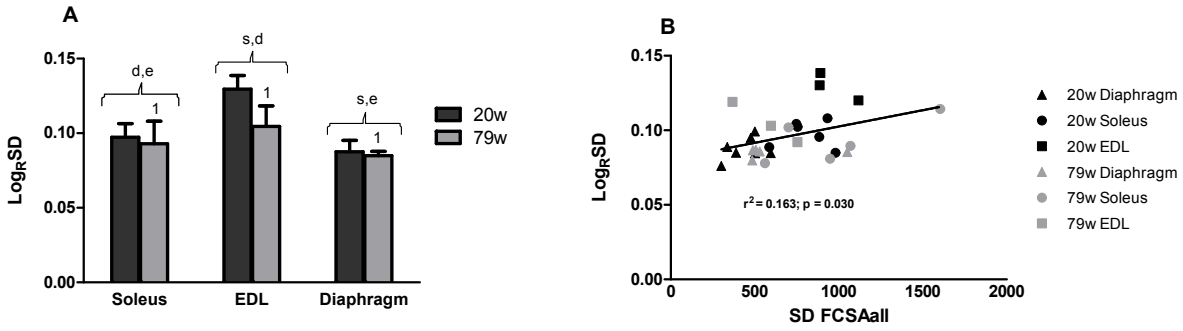
A
0.15
0.10
0.05
0.00
LogRSD
d,e
1
s,d
1
s,e
1
Soleus
EDL
Diaphragm
20w
79w
B
0.15
0.10
0.05
0.00
LogRSD
r2= 0.163; p = 0.030
0
500
1000
1500
2000
SD FCSAall
20w Diaphragm
20w Soleus
20w EDL
79w Diaphragm
79w Soleus
79w EDL

Figure 5

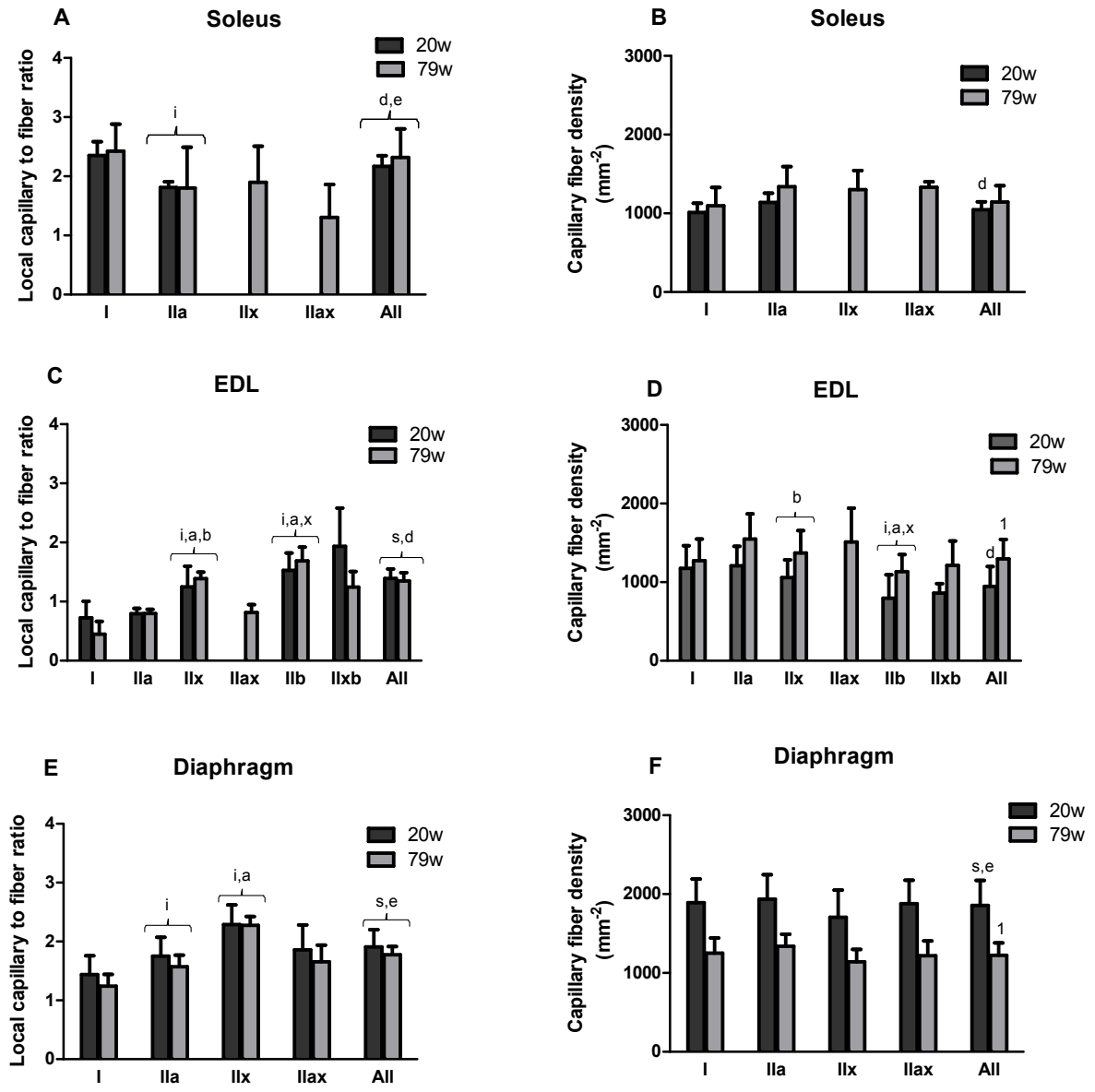
A
Soleus
20w
79w
Local capillary to fiber ratio
i
d,e
I
IIa
IIx
IIax
AII
B
Soleus
Capillary fiber density (mm-2)
d
C
EDL
i,a,b
i,a,x
s,d
IIb
IIxb
D
EDL
b
1
E
Diaphragm
i,a
s,e
F
Diaphragm

Figure 6

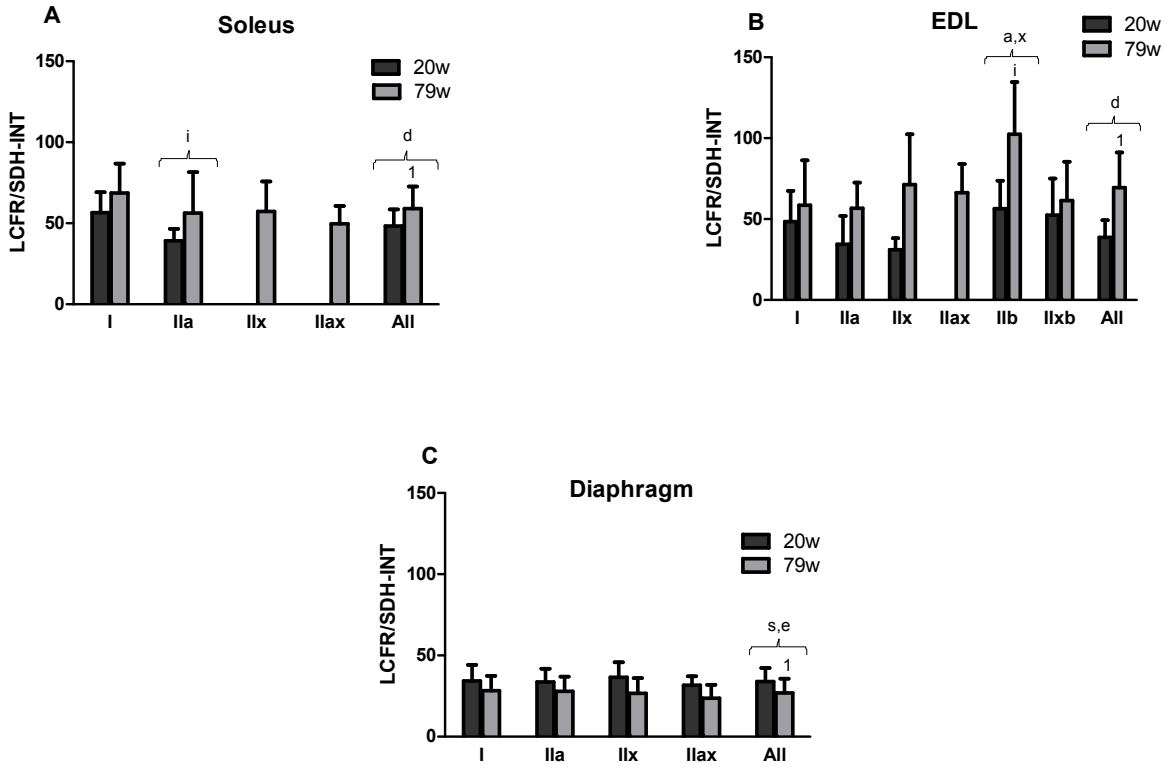
A
Soleus
LCFR/SDH-INT
150
100
50
0
20w
79w
i
d
1
I
IIa
IIx
IIax
AII
B
EDL
a,x
i
d
1
IIb
IIxb
C
Diaphragm
s,e

Figure 7

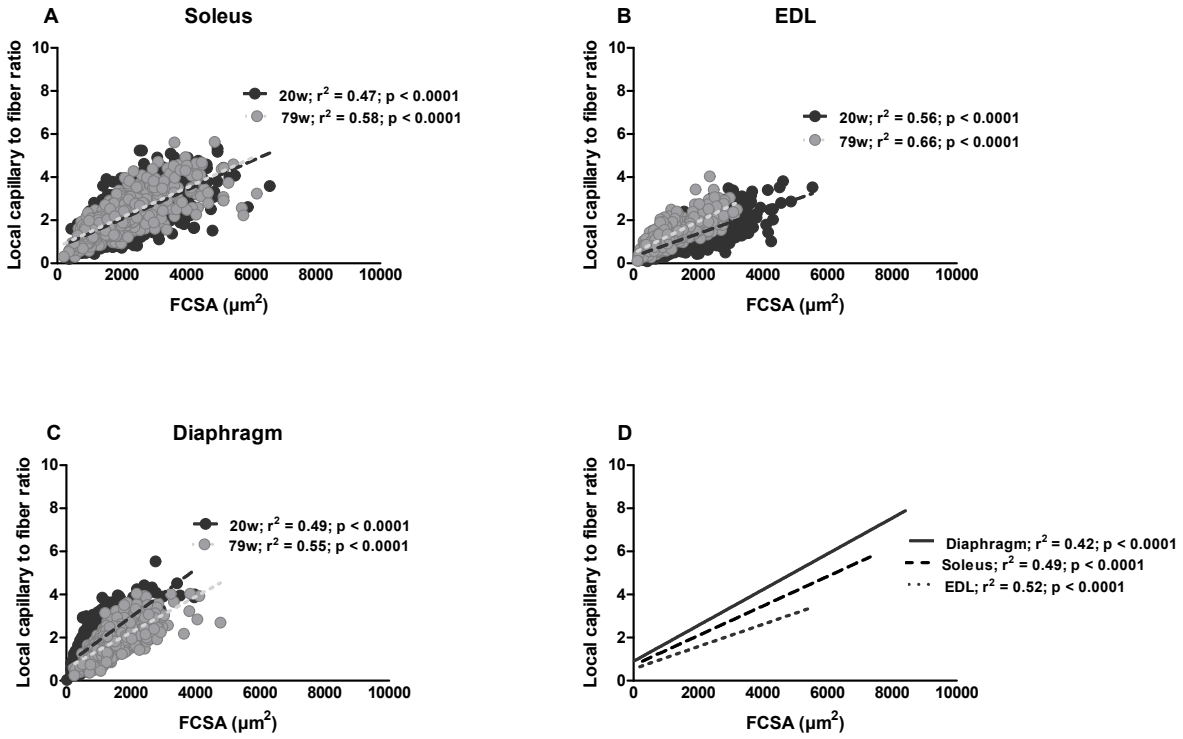
A
Soleus
Local capillary to fiber ratio
FCSA (μm²)
20w; r² = 0.47; p < 0.0001
79w; r² = 0.58; p < 0.0001
B
EDL
20w; r² = 0.56; p < 0.0001
79w; r² = 0.66; p < 0.0001
C
Diaphragm
20w; r² = 0.49; p < 0.0001
79w; r² = 0.55; p < 0.0001
D
Diaphragm; r² = 0.42; p < 0.0001
Soleus; r² = 0.49; p < 0.0001
EDL; r² = 0.52; p < 0.0001

Figure 8